# Supplementary Material
# Land surface controls on afternoon precipitation diagnosed from observational data: Uncertainties, confounding factors and the possible role of vegetation interception

Benoit P. Guillod[1], Boris Orlowsky[1], Diego Miralles[2], Adriaan J. Teuling[3], Peter Blanken[4], Nina Buchmann[5], Philippe Ciais[6], Michael Ek[7], Kirsten L. Findell[8], Pierre Gentine[9], Benjamin Lintner[10], Russell L. Scott[11], Bart Van den Hurk[12], and Sonia I. Seneviratne[1]

[1]ETH Zurich, Institute for Atmospheric and Climate Science, Zurich, Switzerland
[2]University of Bristol, Bristol, UK
[3]Wageningen University, Wageningen, Netherlands
[4]University of Colorado, Boulder, USA
[5]ETH Zurich, Institute of Agricultural Sciences, Zurich, Switzerland
[6]LSCE, Gif-sur-Yvette, France
[7]NCEP/NOAA, USA
[8]GFDL, Princeton, USA
[9]Columbia University, New York, USA
[10]Rudgers, the State University of New Jersey, New Brunswick, USA
[11]USDA-ARS Southwest Watershed Research Center, Tucson, USA
[12]KNMI, Netherlands

September 18, 2013

## S1 North American Regional Reanalysis: sensitivity of EF-precipitation relationship to the time period and to the selection of potentially convective days

Although the NARR product is available from 1979 to present, we use only a subset of the data in order to avoid effects of different time periods for different datasets. Since most of the analyses presented in the main part of this paper includes data from both NARR and the GLEAM-NEXRAD combination, computations are restricted to days when data is available from the GLEAM-NEXRAD combination (years 1995-2007 minus gaps in GLEAM-NEXRAD combination). In order to test the impact of the reduced amount of data from NARR, Figure S1 displays TFS$^{\star}$ computed from NARR using years 1979-2007 (left) and using only years and days with data in the GLEAM-NEXRAD combination (1995-2007 minus some gaps, right). In spite of small, local differences, the overall features remain highly similar when comparing the two resulting maps of TFS$^{\star}$.

In addition, the impact of the criteria for the selection of convective days (see Section 3b) is tested in Figure S2: TFS$^{\star}$ is computed using (left) our radiation-based criteria and (right) the original criteria from Findell et al. (2011). The pattern and the amplitude of TFS$^{\star}$ are highly similar using either criteria. We recall here that the radiation criteria used in this study was chosen in order to allow the use of the same criteria for all datasets, since only few FLUXNET sites are located in the viscinity of radio-soundings, which are necessary for the computation of CTP.

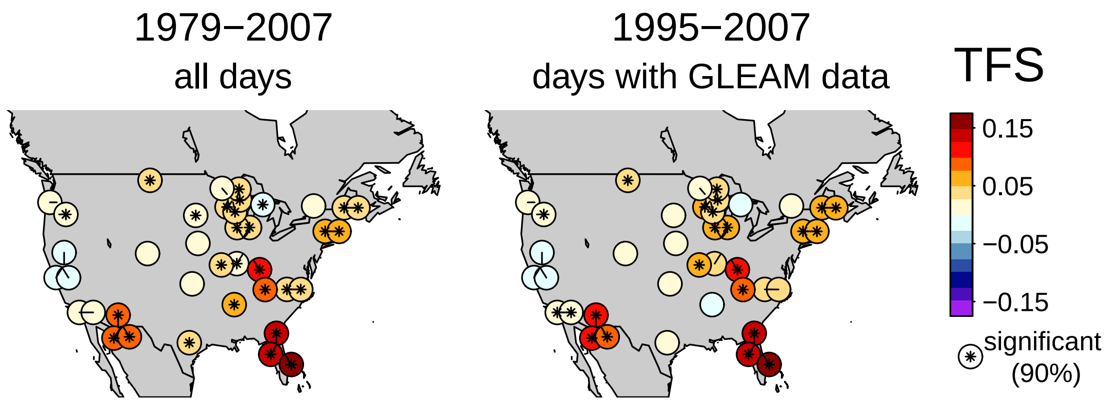


Figure S1: Impact of the time period on the computed impact of EF on convection triggering in NARR: TFS* computed with (left) data from 1979-2007 and (right) with the subset of days when data is also available from the GLEAM-NEXRAD combination (years 1995-2007 minus some periods with gaps). Similar results are found for both subsets of data, highlighting a small impact of the time period on the results.

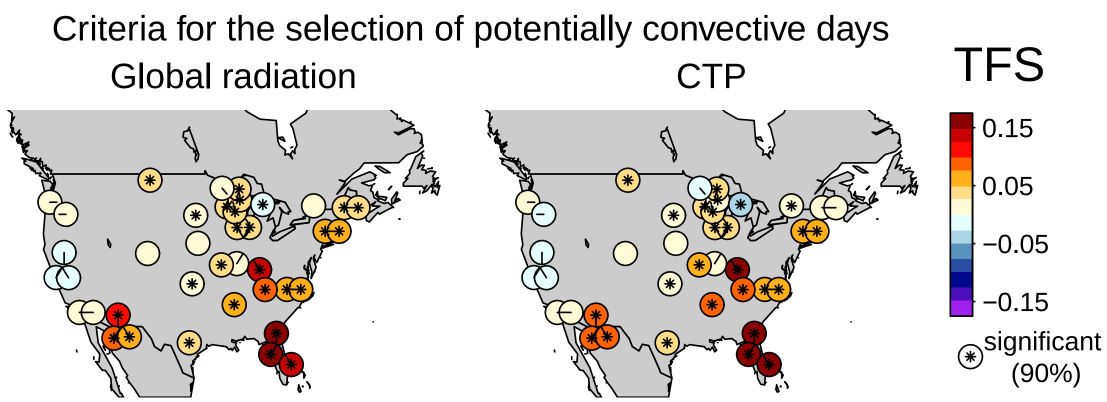


Figure S2: Impact of the selection of potentially convective days on the computed impact of EF on convection triggering in NARR: TFS* computed using (left) our radiation-based criterion and (right) CTP-based criterion from Findell et al. (2011). Days with morning precipitation are removed in both cases. The computation is restricted to 1979-2003 due to readily available CTP data over that period. The resulting maps show that the use of our radiation-based criterion instead of the original CTP-criteria leads to highly similar values of TFS*.

# S2 Sensitivity of GLEAM to the precipitation dataset used as input

As described in the main part of this paper (see Section 2d), GLEAM-derived estimates of before-noon EF are computed using precipitation from NEXRAD as input. To test the sensitivity of our results to the choice of precipitation dataset in the GLEAM computation, we repeated the experiment by replacing NEXRAD precipitation with precipitation from the CPC Unified Gauge Product (Chen et al., 2008) and from PERSIANN (Hsu et al., 1997), two products that match the required timing described thoroughly in Section 2d. Figure S3 shows the Triggering Feedback Strength computed with these three version of the GLEAM product, where for the TFS computation NEXRAD precipitation is used in all cases. As can be clearly seen, while there are differences in the strength and significance of TFS, all three estimates display some coupling in the Eastern USA, giving us confidence in the robustness of our GLEAM-based results with respect to precipitation input.

Table S1 shows the definition of days for two common daily precipitation datasets: CPC-Unified (Chen et al., 2008) and GPCP-1DD (Huffman et al., 2001). While GPCP-1DD has a clearly defined timing that is consistent globally, it does not fit our experimental setting with GLEAM, since precipitation during roughly the 12 hours preceding the estimated EF would be missed. CPC-Unified, on the other hand, fits our requirements over the US (day ending in the morning), although one cannot exclude that afternoon precipitation is included due to possibly different reporting times between different PIs. Thus, in order to exclude any confounding effect due to the mentioned issues, we restricted the analyses in the main part of the paper to a version of GLEAM derived using precipitation from NEXRAD.

Table S1: Definition of the day (timing) for the discussed precipitation datasets. PERSIANN and NEXRAD are available at a 3-hourly resolution and are used in the analysis. Two common daily precipitation datasets, CPC-Unified and GPCP-1DD are described as follows: For precipitation on day ($i$), the timing definition in UTC and US local time are shown. The US local timings for the West coast and the East coast are expressed in standard time (i.e., local time without the offset for daylight saving time).

| **Dataset** | **Timing definition (UTC) for day $i$** | **US local timing West (East) coast** | **Reference** | **Shown in** |
|---|---|---|---|---|
| CPC-Unified | Country-dependent USA: from 12z, day $(i-1)$ to 12z, day $(i)$ | 4AM (8AM), day $(i-1)$ to 4AM (8AM), day $(i)$ | Chen et al. (2008) | Figure S3 |
| GPCP-1DD | UTC day (0z-0z) | 4PM (8PM), day $(i-1)$ to 4PM (8PM), day $(i)$ | Huffman et al. (2001) | not suited |
| PERSIANN | 3-hourly resolution | | Hsu et al. (1997) | Figure S3 |
| NEXRAD | 3-hourly resolution | | `http://www.ncdc.noaa.gov/oa/radar/radarresources.html` | main paper |

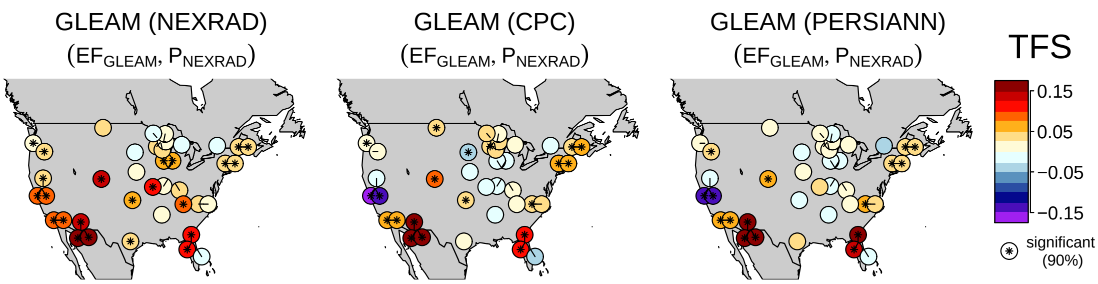


Figure S3: Triggering Feedback Strength (TFS) based on remote-sensing products (GLEAM, NEXRAD) where EF is computed using different precipitation datasets as input (from left to right: NEXRAD, CPC, PERSIANN). All 3 versions display positive coupling in the Eastern USA, albeit with different amplitude and significance. Note that precipitation from NEXRAD is used for TFS computation for all three datasets.

# S3 EF Correlations at longer time scales

Figure 4 in the main part of this paper highlights weak correlations between before-noon EF estimations from different datasets. Figure S4 display correlations of 10-days and monthly means of before-noon EF values. Values are higher than using daily values of before-noon EF, which suggest large uncertainties in EF on short time-scales. Nonetheless, correlations remain small, mostly around 0.5, highlighting uncertainties in EF even on longer time scales. Using EF anomalies instead of absolute values lead to similar results, albeit with slightly lower correlations (not shown).

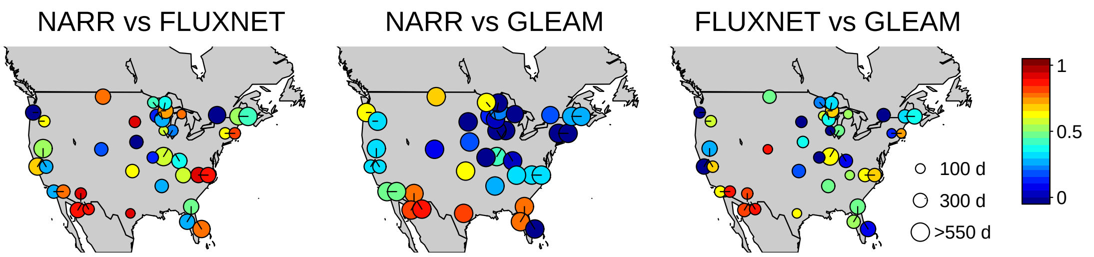


(a) 10 days

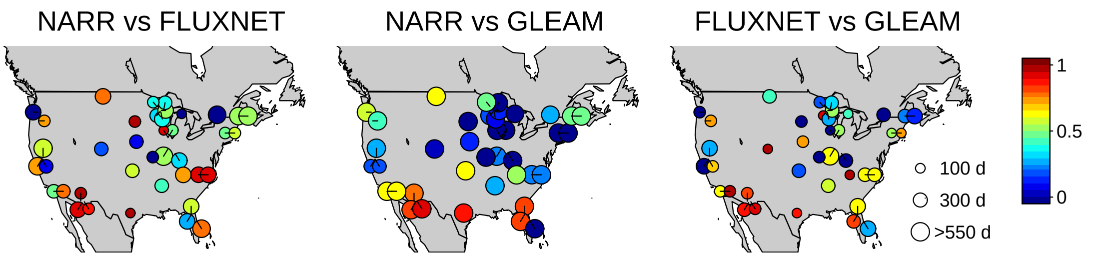


(b) monthly

Figure S4: Correlation of JJA before-noon EF values between different datasets, using EF averages over different time scales: (a) 10-days averages (b) monthly averages. Although correlations are larger than for daily values (Figure 4 in the main paper), they mostly remain low. The size of the dots indicates the number of days included in the computation according to the legend shown on the bottom right map.

## References


Chen, M., W. Shi, P. Xie, V. B. S. Silva, V. E. Kousky, R. Wayne Higgins, and J. E. Janowiak. 2008. Assessing objective techniques for gauge-based analyses of global daily precipitation. *J Geophys Res* **113**, D04110.

Findell, K. L., P. Gentine, B. R. Lintner, and C. Kerr. 2011. Probability of afternoon precipitation in eastern United States and Mexico enhanced by high evaporation. *Nature Geosci* **4**, 434–439.

Hsu, K.-l., X. Gao, S. Sorooshian, and H. V. Gupta. 1997. Precipitation estimation from remotely sensed information using artificial neural networks. *J Appl Meteorol* **36**, 1176–1190.

Huffman, G. J., R. F. Adler, M. M. Morrissey, D. T. Bolvin, S. Curtis, R. Joyce, B. McGavock, and J. Susskind. 2001. Global precipitation at one-degree daily resolution from multisatellite observations. *J Hydrometeorol* **2**, 36–50.